# Analysis of a Heat Exchanger Coil Tube in a Petrochemical Reactor After Fire

Serdar Karakaş*

*Technical Education Faculty, Department of Metal Education, Suleyman Demirel University, 32260 Isparta, Turkey*

(Received June 21, 2010)

## ABSTRACT

The paper is focused on the estimation of the remaining service life of a centrifugally-cast stainless steel heat exchanger tube component which was exposed to high temperatures during a fire incident. Detailed microstructural analyses and tensile tests were carried out to evaluate the metallurgical condition of the tube. The microstructure of the exposed steel was compared to its as-cast counterparts. Coarsened precipitates and secondary precipitation were observed at the grain boundaries. The tensile properties of the specimen exposed to the fire were impaired and the steel was therefore not recommended for further use. The coarsening of the grain boundary precipitates was caused mainly by short-term high-temperature exposure of the steels during the fire.

**Keywords:** Heat-exchanger failures, corrosion, internal carbide formation, steels.

*Corresponding author. Tel.: +90 246 211 1474;
Fax: +90 246 237 1283.
E-mail address: serdarkarakas@yahoo.com
(M.S. Karakaş).

## 1. INTRODUCTION

Furnace heat exchanger coil tubes operating in a major petrochemical plant in Izmir, Turkey were greatly damaged after a fire accident. While most of the tube components in the plant were replaced after the fire, some parts that did not show visual signs of damage were welded to the new (substituted) component materials.

Carbon steel, which is widely used in the industry, loses its usefulness above about 773 K (500°C) due to creep, strength degradation and corrosion. Alloy steels, with enhanced creep/corrosion properties for high temperature applications have been developed since the beginning of the $20^{th}$ century. The petrochemical industry has been using centrifugally cast stainless steels with high chromium and nickel additions (with nominal Cr and Ni content of 25 mass % and 20 mass %, respectively) in reformer and pyrolysis furnaces since the 1960s /1/. The addition of chromium is crucial for the corrosion resistance of the alloy. Chromium causes a continuously adherent protective layer to be formed at the surface /2/; however chromium is also a ferrite stabilizer, which is the reason why nickel, an austenite stabilizer, must also be added to counterbalance this effect. The as-cast microstructure of these steels generally consists of an austenite matrix with chromium carbides of $Cr_7C_3$ type at interdendritic locations. During creep, these carbides may gradually transform to $Cr_{23}C_6$ type /3/. Over the years, additions of

niobium, tungsten, and titanium were made to further enhance the creep strength, creep ductility, and carburization resistance /4-9/. These additions lead to the secondary precipitation of carbides with lower metal-to-carbon ratios, and they have significantly expanded the useful temperature range of these steels for high temperature applications.

In the current study, the Manaurite XM-grade entrance tubes of the heat exchanger were studied. The Manaurite alloys are a development of the high temperature HP-type steels with additions of titanium and niobium. Titanium combines with carbon in the steel, forming carbides that lead to an improvement in the creep strength and toughness at high temperatures. Niobium combines with carbon to form NbC in the form of fine, stable precipitates, increasing the creep strength. Niobium is also known to cause fragmentation in the primary carbide network, minimizing creep crack growth /10/. Each of these two elements is added to the steel generally in an amount of less than 0.1 wt.%. The Manaurite XM alloy also contains zirconium. Zirconium is also a strong carbide former, which can change the morphology of the carbides in the microstructure /4/.

While the events that occurred during the fire are not perfectly known, local temperatures of up to 1473 K (1200°C) were recorded in the plant during the fire. The failure of furnace tubes can occur in a variety of modes, by the effects of: (i) overheating, (ii) intergranular fracture due to creep deformation and (iii) extensive carburization. In order to determine the remaining service life, the tube components that were not replaced after the incident were investigated by carrying out tensile tests and scanning electron microscopy (SEM) on specimens. The microstructures of the steels exposed to the fire were compared to their as-cast counterparts.

## 2. EXPERIMENTAL

As-cast and exposed steels of centrifugally cast Manaurite XM were obtained from the petrochemical plant. The nominal compositions /11/ of the steel are shown in **Table 1**. The compositions of the steel were verified by optical emission spectroscopy. Metallographic and tensile test specimens were prepared from the exposed steels. Specimens from as-cast steels were also metallographically prepared for comparison.

**Table 1**
The chemical composition of alloy Manaurite XM

| Element | Composition (wt%) |
|---|---|
| Carbon, max | 0.35-0.60 |
| Manganese | 1-1.5 |
| Silicon, min | 1-2 |
| Nickel, max | 33-38 |
| Chromium, max | 23-28 |
| Add. Alloy. Elem. | Nb, Ti, Zr |

The outer diameter and wall thickness of the tube was 80 mm and 7 mm, respectively. Three metallographic specimens were obtained from the steels by cutting cross-sectional specimens perpendicular to the pipe axis using a water-cooled abrasive cutter. The specimens were prepared for microscopy using conventional grinding/polishing procedures until a mirror-polish was obtained. The precipitates in the microstructures were initially observed under an optical microscope in the as-polished state. The microstructures of the specimens were then further examined in detail under a JEOL JSM-6400 Scanning Electron Microscope (SEM) equipped with a NORAN System Six Energy-Dispersive X-ray Microanalysis (EDX) system. Although cross-sections both perpendicular and parallel to the tube axis were prepared, only perpendicular cross-sections will be shown in this report, as no significant change in microstructure was observed with orientation.

Tensile test specimens parallel to the tube axis were prepared and tested in accord with the ASTM E8M standard, "Tension Testing of Metallic Materials". A 60-ton capacity ALŞA Tension-Compression Testing Machine was used for tensile testing. A minimum of three specimens were tested for each batch and the results averaged. The term MANXM shall be used for the Manaurite XM specimen in the remainder of this report.

## 3. RESULTS

### 3.1. As-cast MANXM Tubes

Specimens from the as-cast tubes of MANXM were initially studied for comparison purposes. The secondary electron images for the as-cast MANXM tube, prepared from a cross-section perpendicular to the pipe axis, are shown in **Figure 1**. The microstructure is austenitic, with fine precipitates located along the grain boundaries. The intergranular precipitates are occasionally interconnected. No distinct difference in grain size was observed between regions near the outer surface and regions near the inner surface.

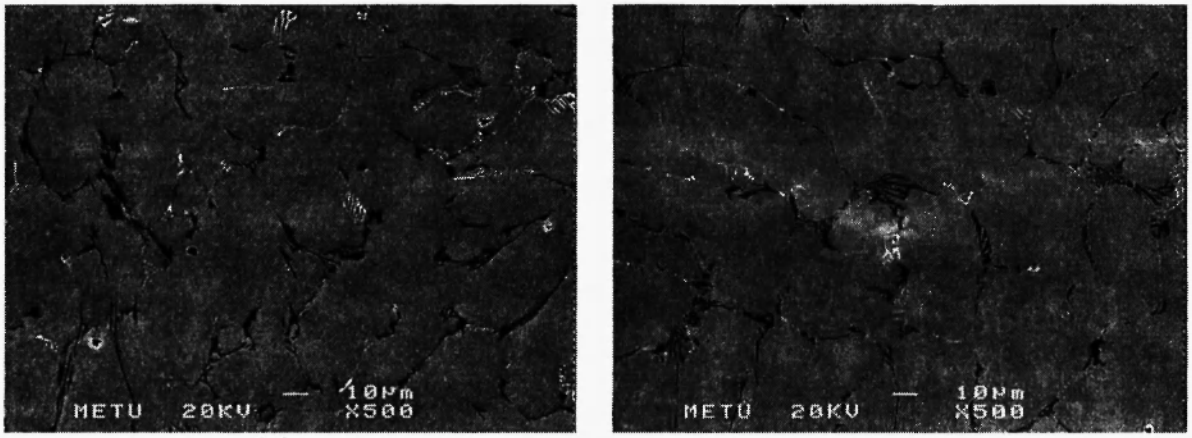


(a) (b)

**Fig. 1:** Microstructure of as-cast MANXM specimen near: (a) the outer surface and (b) the inner surface of the tube (from a cross-section perpendicular to the tube axis).

A higher magnification micrograph of the specimen is shown in **Figure 2.** Three distinct particles, marked "A", "B" and "C" on the figure are identified. The precipitate showing dark contrast, marked "A" in **Figure 2(a)** was initially assumed porosity, but the backscattered image in **Figure 2(b)** clearly indicates that the particle is in fact a precipitate of low atomic number.

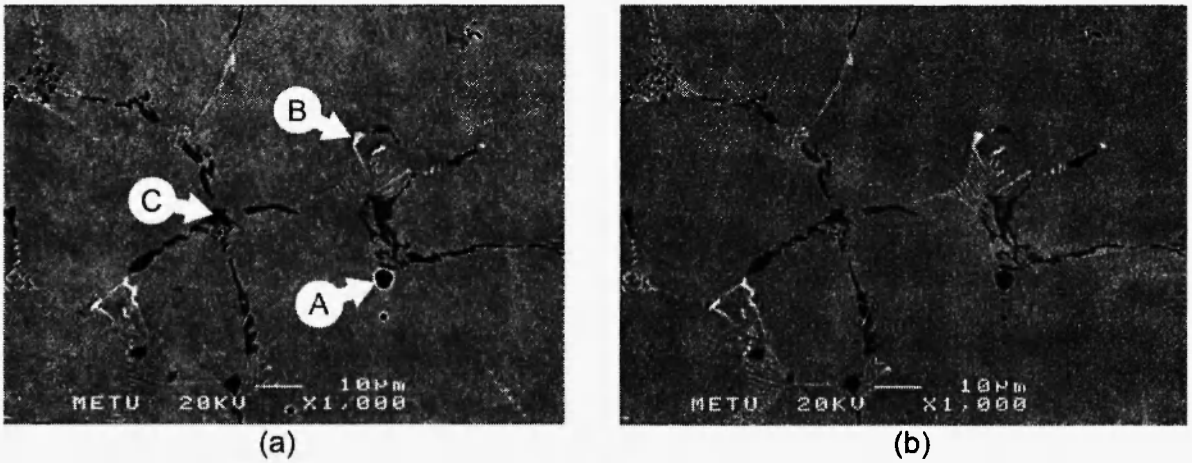


(a) (b)

**Fig. 2:** Higher magnification micrograph of as-cast MANXM specimen showing precipitates: (a) secondary electron image; (b) backscattered electron image.

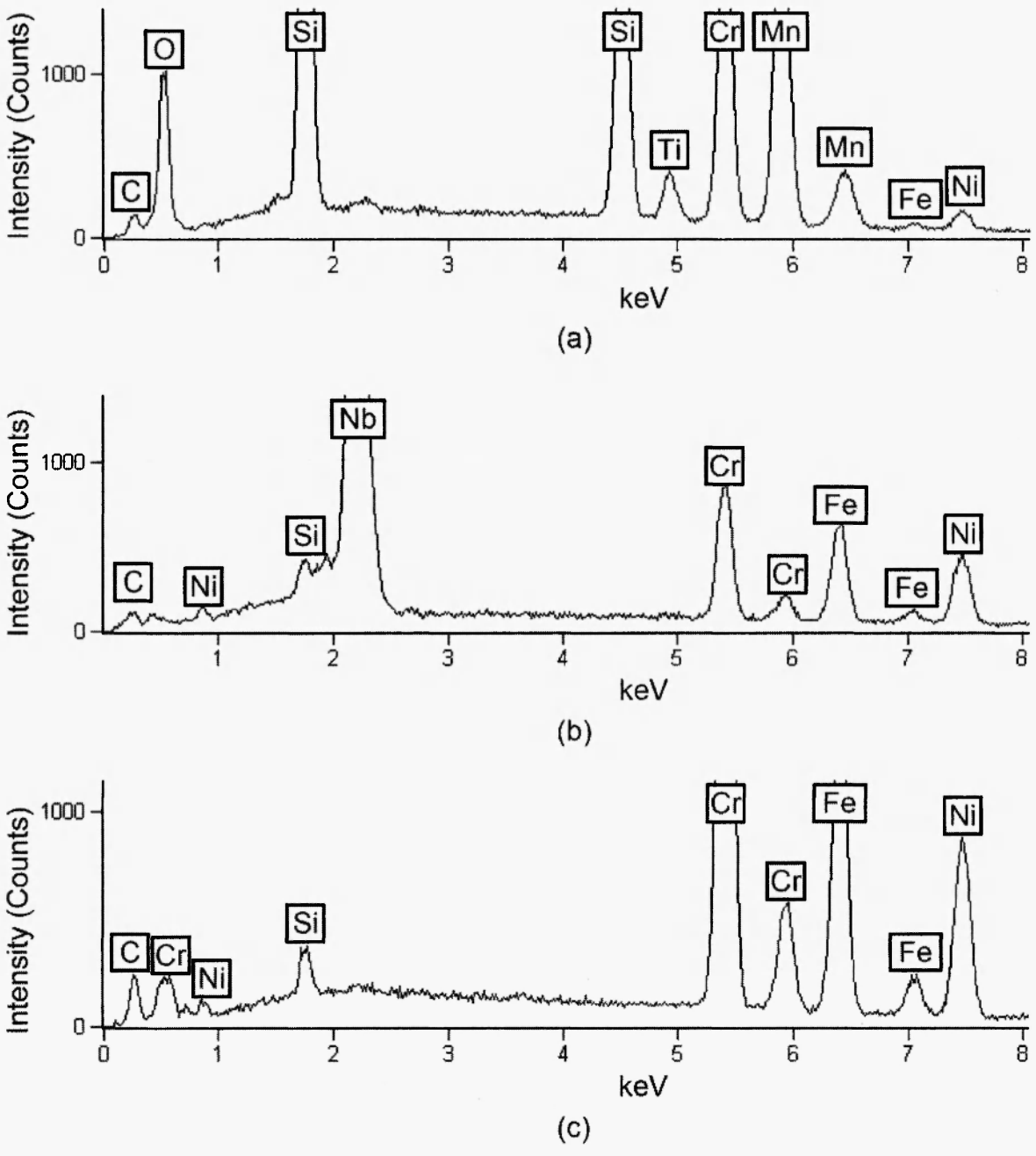


**Fig. 3:** EDX spot analysis spectrum of: (a) point "A"; (b) point "B"; and (c) point "C" of Fig. 2(a).

EDX analyses were conducted on each of the precipitates in order to gather further information with regard to composition. In **Figure 3(a)** is shown an EDX spectrum of the black precipitate "A" indicating that the precipitate is rich in silicon and oxygen content, with relatively high levels of titanium. It is likely that this phase is an inclusion in the alloy, formed as a result of reaction between silicon and impurities in the steel. An EDX analysis of the white precipitate marked "B", **Figure 3(b)**, revealed that the precipitate contained high levels of niobium, silicon and nickel. The dark grey precipitate marked "C" showed high concentrations of

chromium, **Figure 3(c)**. This phase is the most abundant precipitate in the microstructure, and corresponds to the chromium carbides.

### 3.2. Exposed MANXM Tubes

The secondary electron images for the exposed MANXM specimen, prepared from a cross-section perpendicular to the pipe axis, are shown in **Figure 4.** The images show that the microstructure is austenitic, with relatively large, mostly interconnected precipitates lying along the grain boundaries. Secondary precipitation within the grains can also be observed. There was no distinct difference in microstructure between regions near the outer surface and regions nearer to the inner surface.

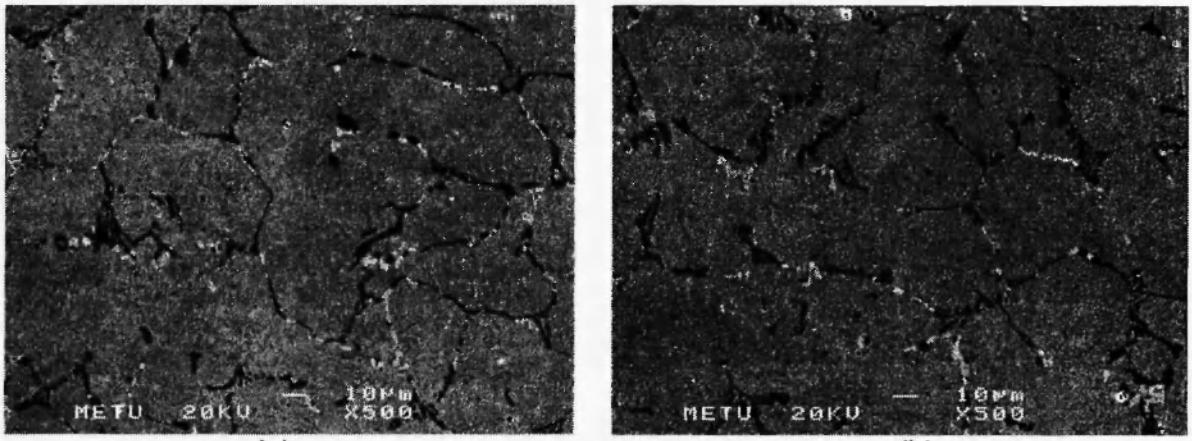


**Fig. 4:** Microstructure of exposed MANXM specimen near: (a) the outer surface and (b) the inner surface of the tube (from a cross-section perpendicular to the tube axis).

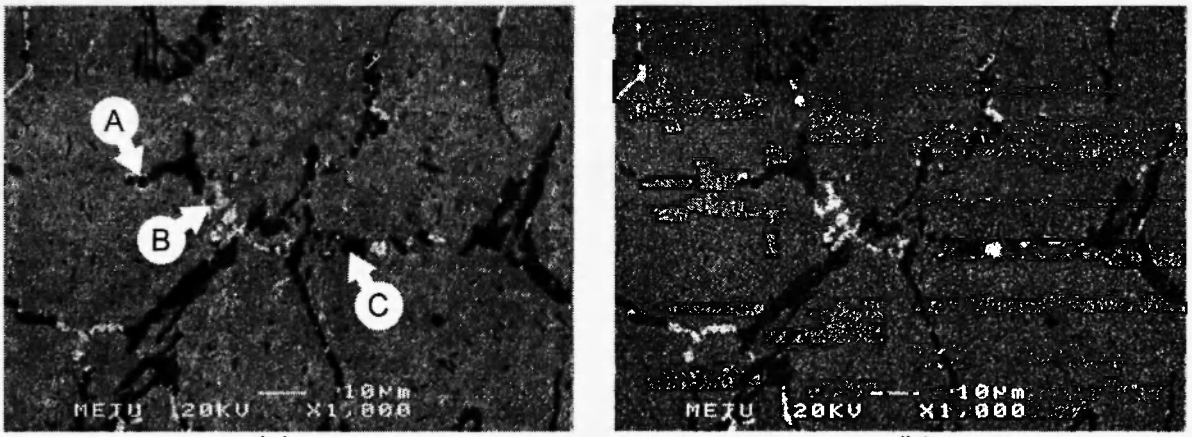


**Fig. 5:** Higher magnification micrograph of exposed MANXM specimen showing precipitates: (a) Secondary electron image; (b) backscattered electron image.

A higher magnification micrograph of the specimen is shown in **Figure 5**, with three distinct precipitates marked as "A", "B" and "C". In **Figure 6(a)** is shown an EDX spectrum of the dark precipitate "A" which indicates that the precipitate is rich in titanium content. Relatively high levels of oxygen are also evident. An EDX analysis of the white precipitate marked "B", **Figure 6(b)**, revealed that the precipitate contained high levels of niobium, silicon and nickel. The dark grey precipitate marked "C" again showed high concentrations of chromium, **Figure 6(c)**.

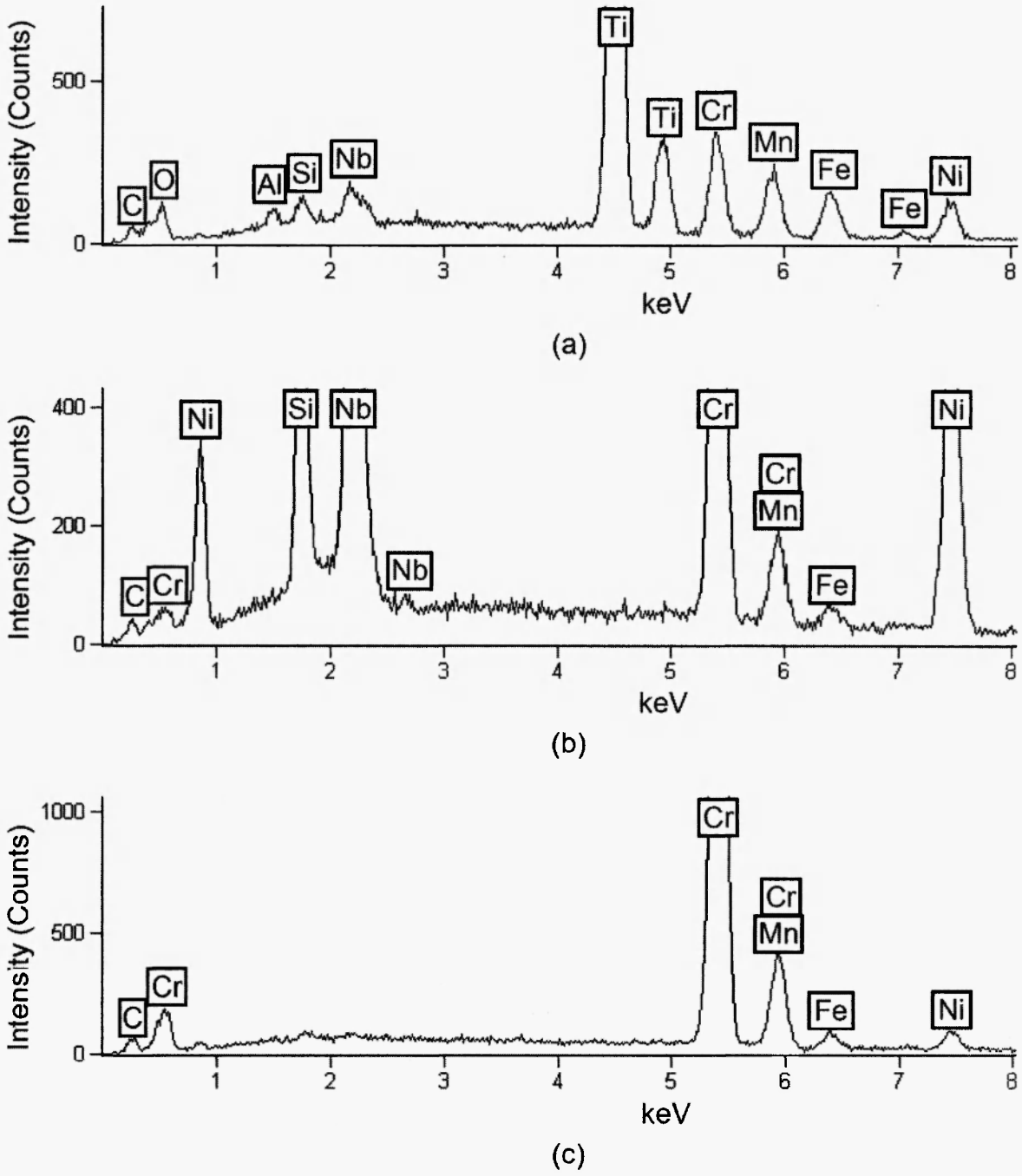


**Fig. 6:** EDX spot analysis spectrum of: (a) point "A"; (b) point "B"; and (c) point "C" in Fig. 5(a)

## 4. TENSILE TESTS

The large number of interconnected precipitates observed at the grain boundaries indicated that the mechanical properties of the exposed heat exchanger tubes would be poor, due to intergranular fracture. The results of the tensile test are shown in **Table 2**. The results given in the table are the average values of three tests. All of the tested specimens failed in a brittle manner, with no observable yield point.

**Table 2**
Ambient-temperature tensile properties of exposed MANXM steel.

| Specimen | Yield Strength, MPa | Tensile Strength, MPa | Elongation, % |
|---|---|---|---|
| MANXM | - | 346 | 0.9 |

Some specimens did not fail between the gage marks and/or failed at regions with greater cross-sectional area, which necessitated the retesting of the specimens. All final elongation values that could be measured were well below two percent.

## 5. DISCUSSION

The microstructures of both the as-cast and exposed heat exchanger tubes were evaluated by scanning electron microscopy. Backscattered electron imaging was useful in the identification of the different precipitates present in the grain boundaries. Detailed elemental analyses of the precipitates were carried out by EDX microanalysis.

The microstructures of the alloy generally consisted of an austenite matrix, with precipitates of chromium and niobium present along the grain boundaries. It is apparent that as chromium carbides grow, excess nickel is rejected into the niobium carbide precipitates, forming niobium-nickel-silicon rich intermetallics /9, 12-13/. This intermetallic is often referred to as the G phase, and the silicon content in the steel is known to promote the NbC $\rightarrow$ G phase transformation /14-16/.

Inclusions rich in titanium and silicon, containing oxygen and sulfur impurities were also detected at the grain boundaries. It is clear that titanium and silicon bind with these impurities, forming spherical precipitates which are less harmful to the mechanical properties of the alloy. Although titanium is a strong carbide former, its carbides were not detected, probably due to the higher affinity of niobium and chromium.

The tube components of the exposed MANXM specimen did not show apparent visual signs of damage via macro-examination. However, the microstructures of the specimen revealed coarsened precipitates at the grain boundaries, as well as secondary precipitation within the austenite grains. Tension tests carried out at room temperature revealed low ductility and tensile strength in the alloy due to grain-boundary precipitation and intergranular fracture. It is clear that the mechanical properties of the exposed specimen were greatly impaired by precipitate coarsening and secondary precipitation, causing brittle failure with less than 2% elongation at room temperature /17/.

While the tension test results only give information regarding room temperature properties, they raised serious doubt concerning the high temperature behavior of the alloy. Due to risks involved with brittle fracture, the tube components were not found suitable for further use.

The main reason for coarsened precipitates occurring at grain boundaries in the exposed heat exchanger tubes is believed to be caused mainly by the short-term exposure to higher than permissible temperatures, which reportedly reached values as high as 1491 K (1218 °C) during the fire. No significant change in grain size was observed between the standard and exposed tubes.

## 6. CONCLUSION

The microstructures of a stainless steel used in the heat exchangers of a petrochemical plant have been studied. Both as-cast and exposed steels have been evaluated and compared in terms of microstructure. The tensile properties of the exposed steel have been determined.

The microstructures of the stainless steel consisted mainly of an austenite matrix with carbide precipitates

in the grain boundaries. Chromium and niobium-rich precipitates have been detected at the grain boundaries, as well as niobium-nickel-silicon rich intermetallics. The exposed steel contained larger and often interconnected precipitates as well as secondary precipitation, which caused significant degradation of the mechanical properties. Room temperature tensile tests showed that the ductility of the overheated specimens were below 2%; for this reason the exposed steel was not recommended for further use in the plant.

Strict temperature control is crucial for the operation of a petrochemical plant in order to avoid catastrophic shutdown. The coarsening of intergranular precipitates and the formation of secondary precipitates within the grains were caused by unacceptably high (~1473 K) temperatures which the steel was exposed to during the fire.

## ACKNOWLEDGEMENTS

The author is grateful to Professor Bilgehan Ögel for his helpful suggestions, comments, and criticisms throughout this study.

## REFERENCES

1. G.D. Barbabela, L.H. Almeida, T.L. Silveira and I. Le May, Phase characterization in two centrifugally cast HK stainless steel tubes, *Mater. Charact.*, **26**, 1-7(1991).
2. J. Harrison, J. F. Norton, R. T. Derricott and J. B. Marriott, *Werkst. Korros.*, **30**, 785-794(1979).
3. H. Wen-Tai and R.W.K. Honeycombe, *Mater. Sci. Technol.*, **1**, 385-389(1985).
4. H.Wen-Tai and R.W.K. Honeycombe, *Mater. Sci. Technol.*, **1**, 390-397(1985).
5. H.M. Tawancy and N.M. Abbas, *J. Mater. Sci.*, **27**, 1061-1069(1992).
6. G.D.A. Soares, H.L. Almeida, T.L. Silveira and I. Le May, *Mater. Charact.*, **29**, 387-396(1992).
7. R.A.P. Ibañez, G.D.A. Soares, L.H. Almeida and I. Le May, *Mater. Charact.*, **30**, 243-249 (1993).
8. J.F. Norton, L. Blidegn, S. Canetoli and D.P. Frampton, *Mater. Corros.*, **32**, 467-478 (1981).
9. G.D. Barbabela, L.H. Almeida, T.L. Silveira and I.L. May, *Mater. Charact.*, **26**, 193-197 (1991).
10. A. Iseda, Y. Sawaragi, F. Masuyama and T. Yokoyama, *Low-alloy heat-resistant steel having improved creep strength and toughness,* U.S. Patent 5211909, (1993).
11. F. Ropital, P. Broutin, M. François and A. Bertoli, *Chromized refractory steel, a process for its production and its uses in anti-coking applications*, U.S. Patent 6348145, (2002).
12. A.A. Kaya, P. Krauklis, and D.J. Young, *Mater. Charact.*, **49**, 11-21(2002).
13. A.A. Kaya, *Mater. Charact.*, **49**, 23-34(2002).
14. F.C. Nunes, L.H. Almeida, J. Dille, J.-L. Delplancke and I. Le May, *Mater. Charact.*, **58**, 132-142(2007).
15. S. Shi and J.C. Lippold, *Mater. Charact.*, **59**, 1028-1040(2008).
16. L.H. Almeida, A.F. Ribeiro and I. Le May, *Mater. Charact.*, **49**, 219-229(2003).
17. K. Guan, H. Xu, and Z. Wang, *Eng. Fail. Anal.*, **12**, 420-431(2005).